PNAS RESEARCH ARTICLE | GENETICS

The ubiquitin–proteasome system regulates meiotic chromosome organization

Xiao Yang[a], Meihui Song[b], Ying Wang[b], Taicong Tan[b], Zhongyu Tian[a], Binyuan Zhai[a], Xuan Yang[a], Yingjin Tan[a], Yanding Cao[b], Shaojun Dai[c], Shunxin Wang[a,d,e,f], and Liangran Zhang[a,b,g,h,1]

Edited by Scott Keeney, Memorial Sloan Kettering Cancer Center, New York, NY; received April 12, 2021; accepted February 25, 2022

Meiotic crossover (CO) recombination is tightly regulated by chromosome architecture to ensure faithful chromosome segregation and to reshuffle alleles between parental chromosomes for genetic diversity of progeny. However, regulation of the meiotic chromosome loop/axis organization is poorly understood. Here, we identify a molecular pathway for axis length regulation. We show that the cohesin regulator Pds5 can interact with proteasomes. Meiosis-specific depletion of proteasomes and/or Pds5 results in a similarly shortened chromosome axis, suggesting proteasomes and Pds5 regulate axis length in the same pathway. Protein ubiquitination is accumulated in *pds5* and proteasome mutants. Moreover, decreased chromosome axis length in these mutants can be largely rescued by decreasing ubiquitin availability and thus decreasing protein ubiquitination. Further investigation reveals that two ubiquitin E3 ligases, SCF (Skp–Cullin–F-box) and Ufd4, are involved in this Pds5–ubiquitin/proteasome pathway to cooperatively control chromosome axis length. These results support the hypothesis that ubiquitination of chromosome proteins results in a shortened chromosome axis, and cohesin–Pds5 recruits proteasomes onto chromosomes to regulate ubiquitination level and thus axis length. These findings reveal an unexpected role of the ubiquitin–proteasome system in meiosis and contribute to our knowledge of how Pds5 regulates meiotic chromosome organization. A conserved regulatory mechanism probably exists in higher eukaryotes.

meiosis | ubiquitin | proteasome | chromosome axis | Pds5

Significance

Meiotic crossover recombination is required for faithful chromosome segregation and promotes genetic diversity by reshuffling alleles between parental chromosomes. Meiotic chromosomes are organized into arrays of loops that are anchored to the proteinaceous axes. The length of the meiotic chromosome axis is intimately associated with crossover frequencies in yeast and higher eukaryotes. However, how chromosome axis length is regulated in meiosis is unknown. Here, we demonstrate that cohesin regulator Pds5 interacts with proteasomes to regulate meiotic chromosome axis length by modulating ubiquitination. This regulatory mechanism also includes two ubiquitin E3 ligases, SCF (Skp–Cullin–F-box) and Ufd4. These findings identify a molecular pathway in regulating chromosome organization and reveal an unexpected function of the ubiquitin–proteasome system in meiosis.

Meiosis is a special process to produce haploid gametes from a diploid precursor cell. Faithful segregation of homologous chromosomes (homologs) of different parents requires the physical connections, crossovers (COs; cytologically visualized as chiasmata), between them. Meiotic COs also promote genetic diversity for evolutionary adaptation (1–3). CO formation is tightly regulated both locally and globally by the meiotic chromosomes, which are organized as linear arrays of loops with proteinaceous axes at their base (1–7). The CO frequency appears to be tightly correlated with axis length (4, 8–11). Moreover, within single meiotic nuclei, axis lengths of all chromosomes vary coordinately, which correlates with per-nucleus CO covariation (9). Therefore, it is of great interest to understand how the meiotic loop/axis is regulated.

Meiotic cohesin is required for the formation of chromosome axes and has been proposed to regulate chromosome loop size and thus axis length (12–16). Pds5 (precocious dissociation of sisters 5) is a key regulator of cohesin and also an axis component (17, 18). The meiosis-specific depletion of Pds5 impairs homolog pairing and leads to dramatically shortened chromosome axes and decreased recombination frequency (19–24). A recent study revealed that Pds5 regulates chromosome axis length in a dosage-dependent manner without altering cohesin abundance (24). However, how Pds5 regulates meiotic chromosome axis length still remains poorly understood.

The 76-residue polypeptide ubiquitin and the small ubiquitin–like moiety (SUMO) are highly conserved in eukaryotes. Both ubiquitin/proteasomes and SUMO are detected abundantly along meiotic chromosomes. They function in multiple processes during meiosis, including homologous chromosome pairing, synapsis, recombination, and chromosome segregation (e.g., refs. 25–30). Antagonistic roles between ubiquitination and sumoylation have been indicated, e.g., in the CO formation process (e.g., ref. 29). Ubiquitination, especially histone H2B monoubiquitination (on lysine 123 in yeast or lysine 120 in mammals) catalyzed by E3 ubiquitin ligase (Bre1 in yeast or RNF20/RNF40 complex in mammals), has already been suggested to regulate chromatin relaxation in both mitosis and meiosis (e.g., ref. 31). However, whether ubiquitin/proteasomes and SUMO are involved in meiotic chromosome loop/axis organization or its regulation is unknown.

In this study, we found that Pds5 interacts with proteasomes and meiosis-specific depletion of Pds5 or proteasomes resulted in accumulated protein ubiquitination and a

Author contributions: Xiao Yang, S.W., and L.Z. designed research; Xiao Yang, M.S., Y.W., T.T., Z.T., B.Z., Xuan Yang, Y.T., Y.C., and S.D. performed research; S.D., S.W., and L.Z. contributed new reagents/analytic tools; Xiao Yang, S.W., and L.Z. analyzed data; and Xiao Yang, S.W., and L.Z. wrote the paper.

The authors declare no competing interest.

This article is a PNAS Direct Submission.

[1]To whom correspondence may be addressed. Email: zhangliangran@sdu.edu.cn.

This article contains supporting information online at http://www.pnas.org/lookup/suppl/doi:10.1073/pnas.2106902119/-/DCSupplemental.

Published April 19, 2022.

short chromosome axis. Further study showed that these defects could be largely rescued by the absence of an ubiquitin-encoding gene *UBI4* or coordinate loss of two E3 ligases SCF (Skp–Cullin–F-box) and Ufd4. These findings establish a molecular pathway of cohesin–Pds5–ubiquitin/proteasome in regulating meiotic chromosome axis length and reveal a previously unknown role for the ubiquitin–proteasome system in this process. This regulatory mechanism is likely conserved in multicellular eukaryotes.

Results

Pds5 Interacts with Proteasomes during Meiosis. Chromosome axes are significantly shorter in Pds5 depletion mutants in meiosis (19–23). To elucidate how meiotic chromosome axis length is regulated, immunoprecipitation–mass spectrometry (IP-MS) experiments were performed to identify new factors that interact with Pds5 (*SI Appendix*, Fig. S1 *A* and *B*). IP-MS from protein extracts of pachytene arrested cells (8 h in sporulation medium [SPM] in an *ndt80*△ background) identified the well-known Pds5 interactors (e.g., cohesin) and a number of potential interactors with high fidelity, including 30 of 33 proteasome subunits (*SI Appendix*, Fig. S1*C* and Dataset S1). An interaction between axis proteins and proteasomes has recently been identified in mouse spermatocytes (32).

The ubiquitin–proteasome and SUMO-modification systems have important roles in meiosis (e.g., refs. 25–29). To confirm the interaction between Pds5 and proteasomes, yeast two-hybrid (Y2H) experiments were performed, which revealed that Pds5 could interact with three subunits of the 26S proteasomes: Pre1 (the β4 subunit of the 20S core particle of proteasomes), Rpn6 (a non-ATPase regulatory subunit of the 19S proteasome lid), and Rpt2 (one of six ATPases of the 19S regulatory particle) (Fig. 1*A* and *SI Appendix*, Figs. S2 and S3 *A* and *B*). The interactions between Pds5 and Pre1 or Rpn6 were further examined by coimmunoprecipitation (Co-IP) experiments performed in yeast meiotic extracts (5 h in SPM) from strains bearing *PDS5-13MYC* in combination with either *PRE1-3FLAG* or *RPN6-3FLAG*. These tagged strains grew well in the yeast extract peptone dextrose medium (YPD) and showed normal meiotic progression, sporulation efficiency, and spore viability (*SI Appendix*, Fig. S4). Each of the two tagged proteasome subunits and the tagged Pds5 could pull down each other (Fig. 1 *B* and *C* and *SI Appendix*, Fig. S3 *C* and *D*). However, we failed to construct a tagged Rpt2 strain or get an appropriate antibody against Rpt2, which prevented us from further examining the interaction between Pds5 and Rpt2 by Co-IP experiments.

Pds5 and Proteasomes were easily detected on meiotic chromosomes by immunostaining (Fig. 2*A* and *SI Appendix*, Fig. S5) (24, 27). The colocalization between Pds5 and proteasomes on chromosomes was examined during prophase I (Fig. 2*A* and *SI Appendix*, Fig. S5). The possible interdependent localization for Pds5 and proteasomes on meiotic chromosome axes was also examined in meiosis-specific depletion of Pds5 or proteasome mutants, where the native promoter was replaced by a mitosis-specific *CLB2* promoter (*pds5-md*, *pre1-md*, or *rpn6-md*) (Fig. 2 *B* and *C*). The substage for each nucleus during meiotic prophase I was judged based on the morphology of Zip1, the transverse filament of the synaptonemal complex (SC) (Fig. 2 *A*–*C* and *SI Appendix*, Fig. S5) (24, 27). Zip1 signal first appears and is visualized as multiple dots at leptotene and as short lines at zygotene, and finally spreads to full lengths of homologs at pachytene, whose contour length also represents the axis length at pachytene (e.g., ref. 33). From preleptotene

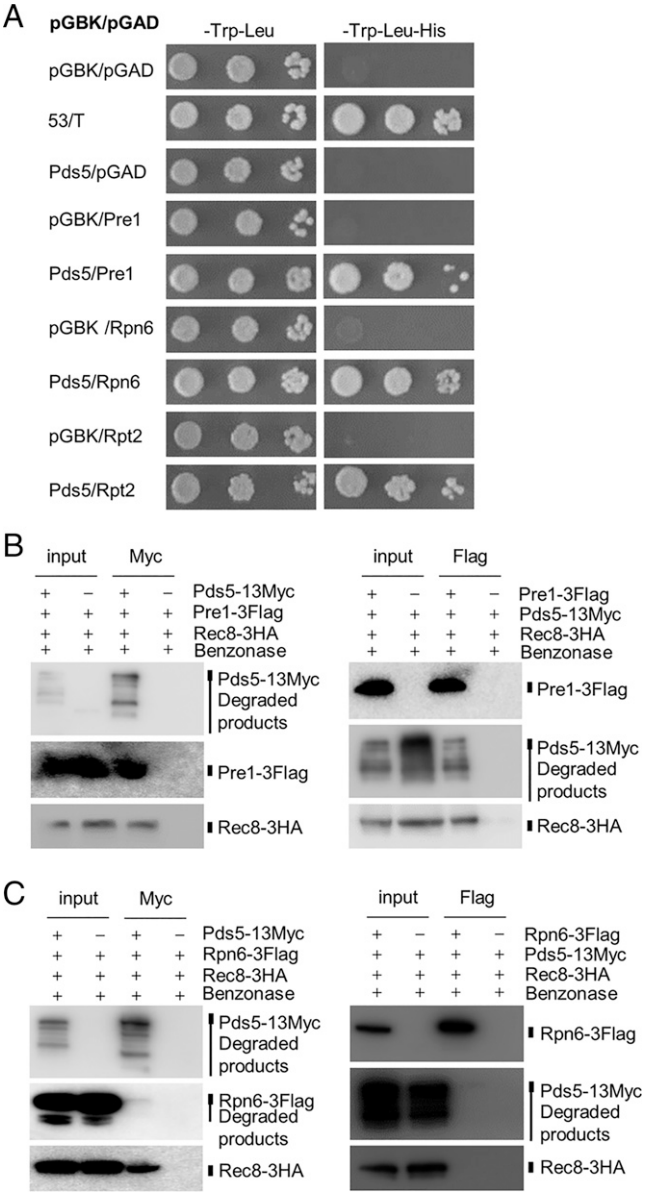

Fig. 1. Pds5 interacts with proteasomes during meiosis. (*A*) Pds5 (in the pGBK vector) interacts with proteasome subunits Pre1, Rpn6, and Rpt2 (in pGAD vectors) in yeast two-hybrid experiments. (*B*) Co-IP experiments showed that Flag-tagged Pre1 and Myc-tagged Pds5 could pull down each other from meiotic lysates (5 h in SPM). Pds5 in meiotic lysate is unstable with degraded fragments. (*C*) Co-IP experiments showed that Flag-tagged Rpn6 and Myc-tagged Pds5 could pull down each other from meiotic lysates (5 h in SPM). Antibodies against the Flag or Myc tag were used. Benzonase endonuclease was added into the IP lysis buffer for all Co-IP experiments to exclude DNA-mediated indirect interactions. The cohesin subunit Rec8 was used as a quantitative control. Experiments were repeated twice.

to pachytene, proteasomes were visualized on chromosomes as multiple foci as revealed by immunostaining of Pre1 (~11 foci per nucleus at preleptotene and ~30 foci from leptotene to pachytene) (Fig. 2 *A* and *D*). Two other proteasome subunits (green fluorescent protein (GFP)-tagged Pup2 and Flag-tagged Rpn6) were also visualized as foci on chromosomes (*SI Appendix*, Fig. S6) (27). Pds5 was detected as foci on chromosomes at preleptotene (before Zip1 appears; ~63 foci per nucleus) and leptotene (~86 foci) (Fig. 2 *A* and *E*). Then Pds5 was detected as short lines at zygotene and as long lines along the full length of homologs at pachytene (Fig. 2*A*). At preleptotene and leptotene, ~35 to 45% of Pre1 foci colocalized with Pds5 foci and ~15% of Pds5 foci colocalized with Pre1 foci

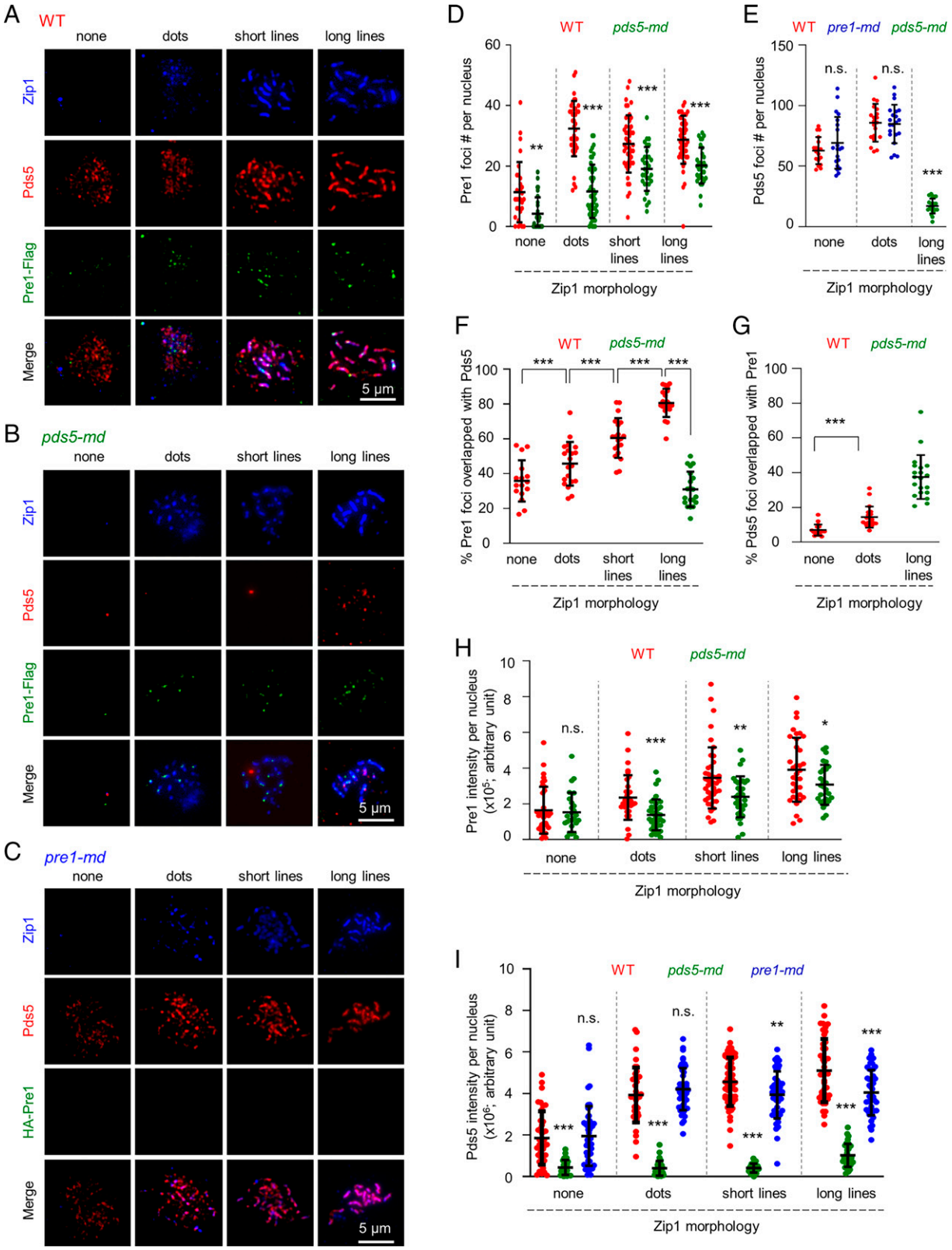

Fig. 2. Partially interdependent colocalization between Pds5 and proteasomes on chromosomes. (*A*–*C*) Representative images of Zip1 (blue), Pds5 (red), and Pre1-Flag/HA-Pre1 (green) staining in WT (*A*), *pds5-md* (*B*), and *pre1-md* (*C*). Meiosis stages were classified according to the morphologies of Zip1 staining: None Zip1 (preleptotene), dot Zip1 (leptotene), short line Zip1 (zygotene), and long line Zip1 (pachytene). Samples were collected at 2 to 5 h (WT) or 2 to 7 h (mutants) in SPM. Antibodies against Zip1, Pds5, and the Flag/HA tag were used. Pre1 foci were undetectable in *pre1-md*. In *pds5-md*, Pds5 foci were detectable at pachytene but not before this stage. (Scale bars, 5 μm.) (*D* and *E*) Quantification of the number of Pre1-Flag (*D*) and Pds5 (*E*) foci. From *Left* to *Right*, n = 30, 30, 40, 49, 46, 30, 47, and 31 nuclei (*D*) and 18, 20, 20, 21, and 20 nuclei (*E*), respectively. (*F* and *G*) Quantification to show the proportion of Pre1-Flag foci overlapped with Pds5-Myc (*F*), and the proportion of Pds5 foci overlapped with Pre1-Flag (*G*). From *Left* to *Right*, n = 16, 20, 20, 20, and 20 nuclei (*F*) and 18, 20, and 20 nuclei (*G*), respectively. (*H* and *I*) Quantification of Pre1-Flag and Pds5 fluorescence intensities. From *Left* to *Right*, n = 35, 26, 33, 37, 34, 31, 35, and 27 nuclei (*H*) and 41, 31, 47, 40, 30, 50, 54, 31, 45, 43, 32, and 45 nuclei (*I*), respectively. Error bar, SD (*D*–*I*). Two-tailed Student's t test (between WT and mutants except specified in *F* and *G*); n.s., not significant ($P \geq 0.05$); *$P < 0.05$; **$P < 0.01$; ***$P < 0.001$.

(Fig. 2 *A*, *F*, and *G*). At zygotene, ∼60% of Pre1 foci colocalized with Pds5, and the frequency increased to ∼80% at pachytene (Fig. 2 *A* and *F*). Since Pds5 was visualized as short or long lines from zygotene to pachytene, its colocalization frequency with Pre1 was not quantified. The increased colocalization frequency between Pds5 and proteasomes is likely caused by the gradual linearity of Pds5 along axes at late stages but less likely at early stages when both Pds5 and proteasomes are visualized as foci.

As expected, Western blots showed that the protein abundance for Pds5, Pre1, and Rpn6 was greatly decreased in *pds5-md*, *pre1-md*, and *rpn6-md* mutants, respectively (*SI Appendix*, Fig. S7 *A* and *B*) (24). Correspondingly, all these mutants showed impaired meiotic progression (*SI Appendix*, Fig. S7 *C*) (24). In *pds5-md*, Pds5 was rarely detectable in nuclei before pachytene and was detected as multiple foci (∼19 foci per nucleus) at pachytene by immunostaining (Fig. 2 *B* and *E*). Interestingly, the number of proteasome foci (Pre1, Pup2, and Rpn6 staining) on chromosomes were also significantly decreased from very early prophase I compared with wild type (WT) (Fig. 2 *B* and *D* and *SI Appendix*, Fig. S6). At pachytene, ∼35% of the residual Pds5 foci (7 among 19 foci per nucleus) still colocalized with Pre1 proteasome foci and ∼31% of Pre1 foci (6 among 17 foci per nucleus) colocalized with Pds5 foci on chromosomes (Fig. 2 *F* and *G*). Consistent with decreased focus number, Pds5 and Pre1 intensities were also significantly decreased in *pds5-md* (Fig. 2 *H* and *I*). In *pre1-md*, Pre1 was rarely detectable on chromosomes although only a moderate decrease was detected by Western blot during prophase I (Fig. 2*C* and *SI Appendix*, Fig. S7 *A* and *B*). Similar Pds5 intensities were observed during early prophase I in *pre1-md* and *rpn6-md* like in WT; however, its intensity was slightly decreased at pachytene in *pre1-md* (Fig. 2 *A*, *C*, and *I* and *SI Appendix*, Fig. S8; Zip1 appears as long lines). These results suggest that Pds5 is at least partially responsible for the recruitment of proteasomes to chromosomes at an early time; however, proteasomes are required to maintain the abundance or stability of Pds5 on chromosomes.

In sum, our above results support the idea that Pds5 can physically interact with proteasomes on meiotic chromosome axes. However, it is worth noting that probably only a fraction of Pds5 interacts with a fraction of proteasomes given their partial colocalization and a moderate decrease of proteasomes on chromosomes in *pds5-md*.

Ubiquitination of Chromosome Proteins Regulates Axis Length. The above results raised the possibility that Pds5 regulates meiotic chromosome axis length via modulating proteasomes. To test this speculation, chromosome axis lengths at pachytene were examined by immunostaining the axis component Rec8 in surface spread nuclei. As reported previously, the cumulative chromosome axis length per nucleus as inferred from the nucleus-wide contour length of Rec8 staining was 43.80 ± 3.16 μm at pachytene (mean ± SD) (Fig. 3 *A* and *B*) (20, 24, 33, 34). However, *pds5-md*, *pre1-md*, *rpt2-md*, and *rpn6-md* single mutants and *pre1-md pds5-md* double mutant showed similarly short chromosome axes (26.51 ± 2.56, 30.35 ± 3.12, 30.29 ± 2.87, 37.78 ± 3.21, and 27.62 ± 3.55 μm, respectively) (Fig. 3 *A* and *B*). The *rpn6-md* and *pre9*Δ (*PRE9* encodes the only nonessential subunit of the core proteasome) showed only a moderate decrease in chromosome axis length probably because the level, assembly, and proteolytic capacity of proteasomes are only moderately affected in these two mutants (Fig. 3 *A* and *B* and *SI Appendix*, Fig. S9) (27, 35). These results suggest that Pds5 can functionally interact with proteasomes to regulate meiotic chromosome axis length in the same pathway.

To further reveal when Pds5 and proteasomes regulate chromosome compaction, the distances between two loci marked with GFP spots on only one of the two chromosome IV were measured in nuclei at different stages judged by Zip1 morphologies (*SI Appendix*, Fig. S10). This analysis showed that more compacted chromosomes were observed from as early as leptotene in both *pds5-md* and *pre1-md* single mutants (*SI Appendix*, Fig. S10). This result suggests that Pds5/proteasomes can regulate axis length from leptotene, probably the time during axis formation, which is consistent with the above conclusion that Pds5 can regulate proteasomes on chromosomes from leptotene.

Proteasomes degrade ubiquitinated proteins. The loss of proteasomes from meiotic chromosomes is expected to accumulate ubiquitinated proteins. Indeed, protein ubiquitination accumulated to high levels in the *pds5-md* and *pre1-md* mutants, although ubiquitination level in *pds5-md* was lower than that in *pre1-md* (Fig. 3 *C* and *D* and *SI Appendix*, Fig. S11). This further raises the possibility that, in the absence of Pds5/proteasomes, the accumulation of protein ubiquitination results in short chromosome axes. If so, decreasing the ubiquitination level in *pds5-md* or *pre1-md* may restore the axis length. Consistent with this idea, deletion of the major ubiquitin coding gene *UBI4* in *pds5-md* or *pre1-md* mutants (the *pds5-md ubi4*△ or *pre1-md ubi4*△ double mutants) decreased ubiquitination to a low level and increased the axis length to nearly WT levels (Fig. 3 *C–F* and *SI Appendix*, Fig. S11). We noted that the *ubi4*△ mutant showed comparable axis length with the *pds5-md ubi4*△ and *pre1-md ubi4*△ mutants (Fig. 3 *C–F* and *SI Appendix*, Fig. S11). This may also suggest neither Pds5 nor the proteasome is required to regulate axis length when there is only a very low level of available ubiquitin. Therefore, these results support the idea that Pds5 and proteasomes work downstream of ubiquitination to antagonize ubiquitination-caused axis shortening during meiosis.

During meiosis, sumoylation also has important roles and may have an antagonistic effect on ubiquitination (26, 29, 30, 34, 36). In *pds5-md*, increased protein ubiquitination was accompanied by decreased sumoylation level (*SI Appendix*, Fig. S12 *A–D*). This raised the question of whether alterations in chromosome axis length result from altered protein sumoylation. To address this possibility, the sumoylation level was increased in the *pds5-md* mutant via copper-induced overexpression of SMT3, which encodes SUMO (*pCUP1-SMT3*). However, the chromosome axis length was not significantly altered under this condition (*SI Appendix*, Fig. S12 *E–G*). This suggests that chromosome axis length is indeed regulated by ubiquitination but not sumoylation. Moreover, chromosomes axis length is maintained unaltered under diverse conditions with significantly increased or decreased sumoylation levels: SUMO-dependent ubiquitin E3 ligase deletion strains with accumulated protein sumoylation (*slx5*△, *slx8*△, and *pds5-md slx5*△ mutants) and a strain with decreased SUMO E2 activity (*ubc9-GFP*) and thus sumoylation (*SI Appendix*, Fig. S12 *F–H*) (26, 34, 36). The result that chromosome axis length is regulated by the ubiquitin/proteasome but not SUMO pathway is also consistent with their different localizations: Ubiquitin/proteasomes primarily localize on chromosome axes while SUMO primarily localizes on the central region of the SC (*SI Appendix*, Fig. S5) (26, 27, 36).

Ubiquitin E3 Ligases Ufd4 and Cdc53 Regulate Chromosome Axis Length. There are ∼100 ubiquitin E3 ligases in budding yeast. We wondered which E3 ligase(s) is responsible for the ubiquitination of chromosome proteins to regulate axis length.

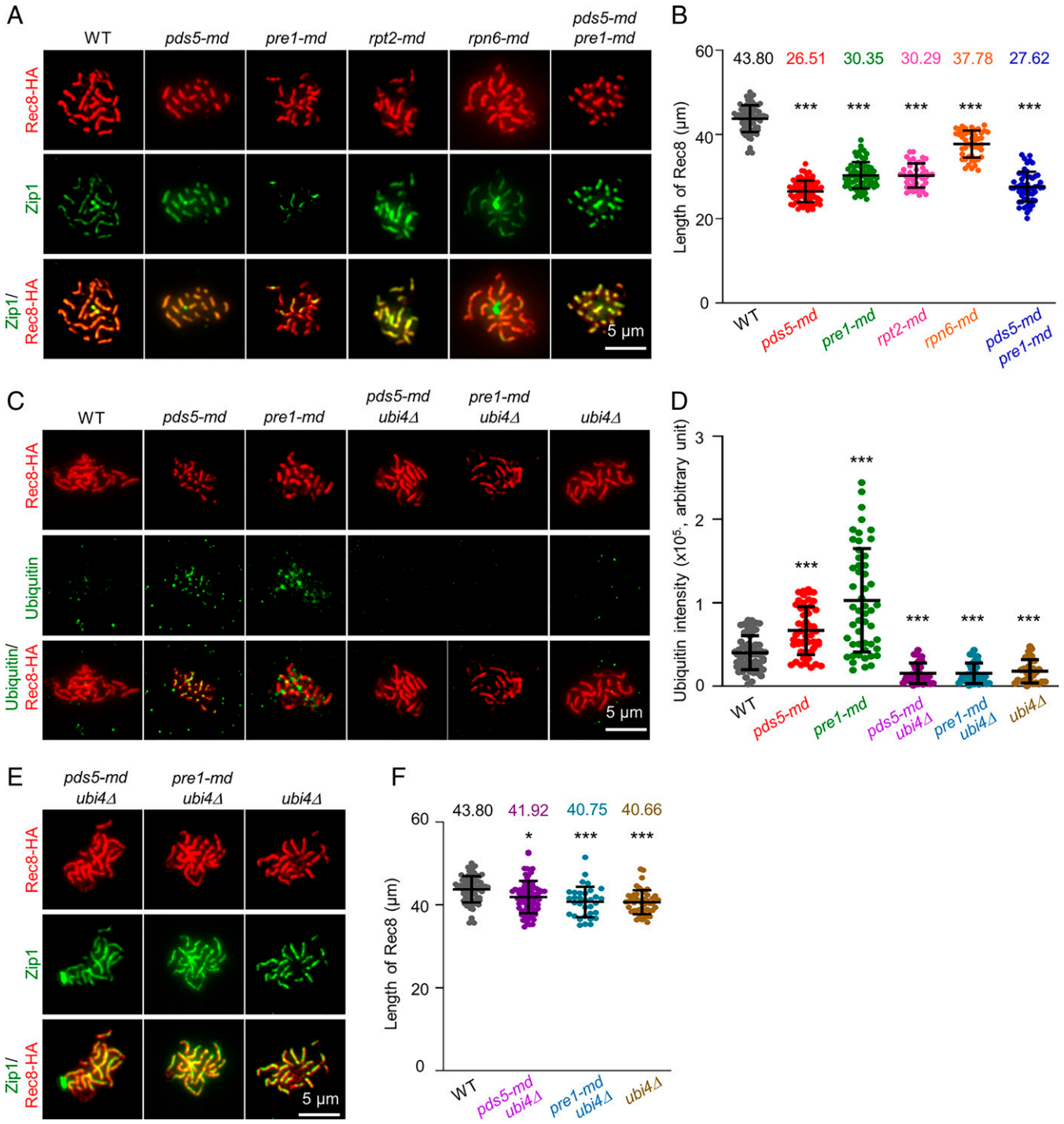

Fig. 3. Pds5 and proteasomes work in the same pathway to regulate chromosome axis length. (*A* and *B*) Representative images of Rec8-HA (red) and Zip1 staining (green) (*A*) and quantification (*B*) to show chromosome axis lengths (Rec8 contour lengths) in pachytene nuclei in the *pds5-md*, *pre1-md*, *rpt2-md*, and *rpn6-md* single mutants, and the *pds5-md pre1-md* double mutant. Data for WT, *pds5-md*, and *pre1-md* were from two independent experiments and combined together since no statistical difference was seen between the two experiments. $n = 81$, 77, 76, 44, 46, and 54 nuclei, respectively. (*C* and *D*) Representative images (*C*) and quantification (*D*) to show protein ubiquitination by immunostaining in pachytene nuclei. $n = 61$, 51, 51, 35, 35, and 30 nuclei, respectively. (*E* and *F*) Representative images (*E*) and quantification (*F*) to show axis length in pachytene nuclei. $n = 81$, 78, 33, and 47 nuclei, respectively. WT data were duplicated from *A* for easy comparison. Samples were collected at 6 to 7 h for *pre1-md* and *rpn6-md* mutants or 10 h in SPM (in *ndt80*Δ background) for other genotypes. Antibodies against Zip1, ubiquitin, and the HA tag were used. (Scale bar, 5 μm in *A*, *C*, and *E*.) Error bar, SD (*B*, *D*, and *F*). Two-tailed Student's *t* test (compared with WT); $*P < 0.05$; $***P < 0.001$.

Our IP-MS experiments identified four ubiquitin E3 ligases (*SI Appendix*, Fig. S1 and Dataset S1). Among them, both Cdc53 and Skp1 are components of a major ubiquitin ligase SCF (Skp–Cullin–F-box). The meiosis-specific depletion of Cdc53 (*cdc53-md*) shows defects in chromosome axis formation, which can be largely rescued by the deletion of the chromosome axis remodeling factor Pch2 (37). This indicates that SCF ligase probably has an important role in regulating chromosome axis length in the ubiquitin/proteasome pathway. When Cdc53 was depleted in *pds5-md* (*cdc53-md pds5-md*), the ubiquitination level was decreased, and the chromosome axis length was also significantly increased by 30% compared with the *pds5-md*

mutant (Fig. 4 and *SI Appendix*, Figs. S11 *C* and *D* and S13 *A* and *B*). This functional interaction is probably mediated by Pds5–proteasome–SCF, since no direct interaction was detected between Pds5 and Cdc53 or Skp1 (*SI Appendix*, Fig. S13*C*).

The other two ubiquitin ligase components identified from our IP-MS experiments are San1 and Ufd4 (*SI Appendix*, Fig. S1 and Dataset S1). To examine their roles in hyperubiquitination in *pds5-md*, deletion mutants were introduced. San1 deletion did not affect chromosome axis length (*SI Appendix*, Fig. S14). When Ufd4 was deleted in *pds5-md*, chromosome axis length was increased by ∼10% compared with *pds5-md* (Fig. 4). When *cdc53-md* and *ufd4*△ were combined in the *pds5-md* background, chromosome axis length was increased by ∼50%, comparable to that in *pds5-md ubi4*△ or *pre1-md ubi4*△ (Figs. 3 *E* and *F* and 4). These results suggest that Cdc53 and Ufd4 are the two major E3 ligases in regulating chromosome axis length. Moreover, these results further support the hypothesis that protein ubiquitination regulates chromosome axis length.

Discussion

In conclusion, Pds5 interacts with proteasomes to regulate ubiquitination and consequently chromosome axis length during meiosis. Moreover, SCF and Ufd4 are the two major ubiquitin E3 ligases involved in this Pds5–ubiquitin/proteasome pathway.

The Cohesin–Pds5–Ubiquitin/Proteasome Pathway Regulates Meiotic Chromosome Organization. Pds5 and proteasomes interact and partially colocalize with each other during meiosis (Figs. 1 and 2). Pds5 likely recruits a fraction of proteasomes to chromosomes during early prophase I. The depletion of either Pds5 or proteasomes or both results in accumulation of ubiquitination and similarly shortened chromosome axes. Both defects can be largely rescued by decreased ubiquitin availability or coordinate loss of two E3 ligases (SCF and Ufd4) (Figs. 3 and 4). Additionally, in the presence of both Pds5 and proteasomes, either increased or decreased ubiquitin availability and thus protein ubiquitination by deletion or overproduction of *UBI4* has little impact on chromosome axis length (Fig. 3 and *SI Appendix*, Fig. S15). These results support a model for Pds5 working with the ubiquitin–proteasome system to regulate chromosome axis length (Fig. 5). First, when there is little ubiquitination (e.g., in *ubi4*△), chromosomes axis length is organized at nearly WT level, which can be considered as a "default" state. Second, ubiquitination of proteins on chromosomes causes axis shortening. Third, Pds5 recruits proteasomes to chromosomes to antagonize ubiquitin-associated axis shortening by removing or preventing a specific fraction of ubiquitination (below). Therefore, Pds5 and proteasomes function during or downstream of ubiquitination as a buffer to keep chromosome axis length constant. This would predict that alterations in the abundance of Pds5 and/or proteasomes would change axis length. This is consistent with our previous finding that the axis length is regulated by the dosage of Pds5 (24).

Our results also raised two important questions. The first question is how chromosome axis length is regulated by ubiquitination. A loop extrusion model has been proposed to explain the organization of the chromatin loop/axis (15, 21, 22, 38, 39). In this model, the central player, cohesin, mediates loop extrusion and Pds5 probably works as a regulator of cohesion. However, alterations in Pds5 have little effect on the level of chromosome-bound cohesin (24). Our current findings show that chromosome protein ubiquitination regulates chromosome axis length. This can be achieved by regulating loop extrusion velocity (e.g., modulating cohesin's loop extrusion activity or chromosome property) or the density/strength of barriers that inhibit loop extrusion.

The second question is when chromosome axis length is regulated by the Pds5–proteasome pathway. In meiosis of many organisms, including budding yeast, mouse, and plants, axis proteins appear on chromosomes before leptotene (e.g., refs. 40 and 41). Lots of axis proteins are recruited to chromosomes by cohesin, which is loaded onto chromosomes during the S phase (e.g., ref. 41). This suggests meiotic chromosome axes probably begin to form soon after DNA replication. Theoretically, axis length can be easily modulated during its formation. Axis length also changes after its formation at least in some organisms (e.g., ref. 42). However, it is unclear whether alterations in overall axis length during prophase I result from global or local changes in loop sizes (see below) or spaces between loops. Pds5 is recruited onto chromosomes by interaction with cohesin before leptotene (24). Cohesin is also an important component of meiotic chromosome axes, whose absence results in disorganized chromosomes (e.g., ref. 21). Moreover, proteasomes are loaded abundantly onto chromosomes during the premeiotic S phase (27). Consistently, cohesin, Pds5, and ubiquitin/proteasomes all primarily localize on chromosome axes rather than

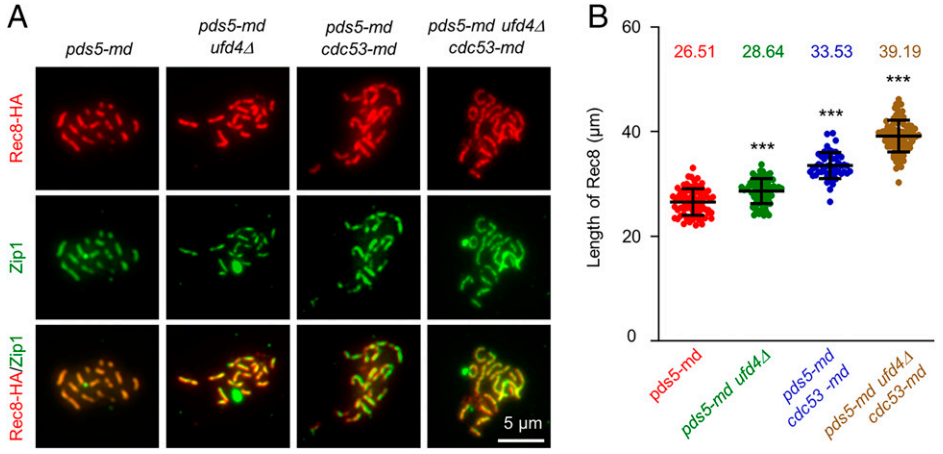

Fig. 4. Ufd4 and Cdc53 are major ubiquitin E3 ligases regulating the chromosome axis. (*A*) Representative images of Rec8-HA (red) and Zip1 (green) staining in *pds5-md*, *pds5-md ufd4*Δ, *pds5-md cdc53-md*, and *pds5-md ufd4*Δ *cdc53-md*. Samples were collected at 10 h in SPM in the *ndt80*Δ background. Antibodies against Zip1 and the HA tag were used. (Scale bar, 5 μm.) (*B*) Quantification of the length of Rec8 in *A*. From *Left* to *Right*, $n = 77$, 69, 50, and 91 pachytene nuclei, respectively. Error bar, SD. Two-tailed Student's *t* test; ***$P < 0.001$ (compared with *pds5-md*).

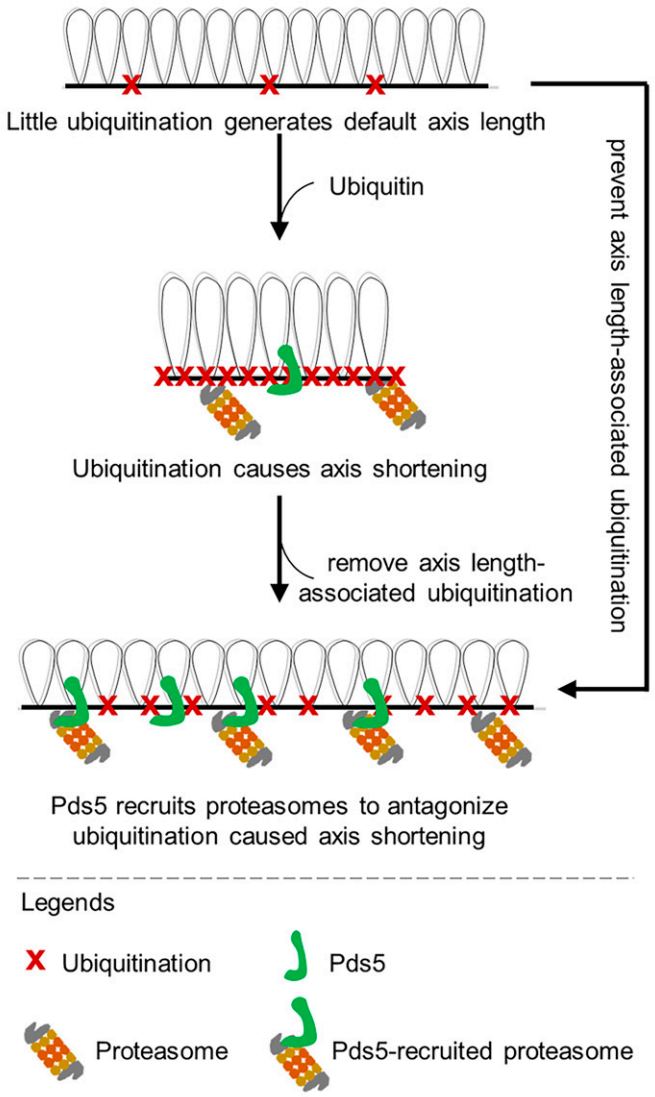

Fig. 5. Illustration of the Pds5–ubiquitin/proteasome pathway in regulating chromosome axis length during meiosis (see text for more details). Meiotic chromosomes are organized as linear arrays of loops anchored to the proteinaceous axes at their base. When there is little ubiquitination (e.g., in *ubi4*Δ), chromosome axis length is organized at a default length regardless of the presence or absence of Pds5–proteasomes. Ubiquitination of proteins on chromosomes results in axis shortening and excessive ubiquitination results in greatly shortened axis, e.g., in the absence of Pds5 and/or proteasomes. Pds5 recruits proteasomes to antagonize ubiquitin-associated axis shortening by removing or preventing the specific fraction of ubiquitination involved in axis regulation.

loops (*SI Appendix*, Fig. S5) (24, 27, 28). Furthermore, more compacted chromosomes are observed from leptotene in *pds5-md* and *pre1-md* mutants compared with WT (Fig. 3 and *SI Appendix*, Fig. S10). These results suggest that Pds5/proteasomes regulate meiotic chromosome axis length more likely during or soon after axis formation.

Our results also show that there is only limited colocalization between pds5 and proteasomes (Fig. 2 *F* and *G*). Moreover, both the number and the intensity of Pre1 foci on chromosomes are only moderately decreased in the *pds5-md* mutant (Fig. 2 *D* and *H*). It is likely that only the Pds5-recruited proteasomes are involved in axis length regulation while the bulk ubiquitination on chromosomes is Pds5 independent and works in other processes, e.g., for proper SC assembly and meiotic exit (27, 28, 32). Consistent with this idea, in the presence of Pds5 and proteasomes on chromosomes, the level of axis length–associated ubiquitination and thus the axis length would be maintained nearly unaltered regardless of the overall hyper- or hypoubiquitination (Fig. 3 *C–F* and *SI Appendix*, Fig. S15). Interestingly, Pds5 intensity on zygotene and pachytene chromosomes is significantly, although slightly, decreased in *pre1-md* (Fig. 2*I*). This raises the possibility that proteasomes have either a direct or indirect role in maintaining Pds5 abundance or stability on chromosomes.

Is the Cohesin–Pds5–Ubiquitin/Proteasome Pathway Conserved? We also wondered whether the Pds5–ubiquitin/proteasome regulation pathway is conserved in multicellular eukaryotes. Pds5 is an important chromosome axis component (19–21, 23). A recent study showed that, as in both budding and fission yeasts, meiotic chromosome axes are shortened to half of the WT level when both PDS5A and PDS5B are depleted in mouse spermatocytes (23). Moreover, both budding yeast and mouse spermatocytes with depleted Pds5 show decreased recombination frequency (it is unclear whether fission yeast with depleted Pds5 has altered recombination frequency) (20, 23, 24). The ubiquitin and proteasomes mainly localize on chromosome axes in budding yeast, *Caenorhabditis elegans*, and mouse (27, 28). Furthermore, the deletion of UBE2B (an ubiquitin E2-conjugating enzyme) results in longer chromosome axes and increased CO frequency in mouse spermatocytes (43). These similarities suggest that a conserved regulatory pathway may exist in mouse to regulate chromosome axis length and recombination frequency. In budding yeast, *Sordaria*, and human meiosis, SUMO primarily localizes on the central region of the SC (36, 44–46). However, in mouse, SUMO mainly localizes on chromosome axes and the bulk axis-associated ubiquitination depends on the axis-associated sumoylation (28). This difference indicates that SUMO may also have an important role in regulating chromosome organization in mouse meiosis.

Materials and Methods

Yeast Strains. *Saccharomyces cerevisiae* strains used in this study are in the SK1 background and described in *SI Appendix*, Table S1.

Meiotic Time Course, Sporulation Efficiency, and Cell Viability. Meiotic time courses were carried out as previously described (24). In brief, yeast cells from −80 °C were patched onto yeast extract peptone glycerol (YPG) plates and incubated at 30 °C overnight. Yeast cells were then streaked onto YPD plates and incubated for 2 d at 30 °C. A single colony was inoculated into YPD liquid medium and incubated at 30 °C for 24 h with shaking. An appropriate amount of YPD cultures was diluted into a presporulation liquid medium and cultured at 30 °C for ∼16 h. Synchronized cells were collected by centrifugation and resuspended in SPM to induce meiosis at 30 °C. At each hour, an appropriate amount of samples was collected, fixed in 40% ethanol, and stained with DAPI to determine meiotic divisions using a fluorescence microscope. For induction of Smt3 (*pCUP1-SMT3*) or Ubi4 (*pCUP1-UBI4*), different concentrations of $CuSO_4$ were added into different aliquots from a single synchronized culture in SPM. Sporulation efficiency was determined as the frequency of cells with asci after 24 h in SPM. Tetrads were dissected onto YPD plates and the percent of viable spores was calculated after 2 d.

Immunoprecipitation and Mass Spectrometry. A TAP-tagged *PDS5* strain in an *ndt80*Δ background was used for IP (a strain without the TAP tag in the same background as a control; the TAP tag consists of a calmodulin binding peptide (CPB), a tobacco etch virus (TEV) protease cleavage site, and Protein A), which was performed as previously described with modifications (47). Briefly, synchronized cells in SPM were collected at 8 h and ground in the presence of liquid nitrogen, and ∼10 g of cells were lysed in 20 mL of lysis buffer (20 mM Hepes/KOH, pH 7.4, 300 mM NaCl, 0.5% Triton X-100, 1 mM dithiothreitol, 0.2 mg/mL phenylmethanesulfonyl fluoride (PMSF), protease mixture [Sigma],

50 mM NaF, 5 mM $Na_4P_2O_7$, 0.1 mM $NaVO_3$). The lysate was incubated with 200 μL IgG Sepharose 6 fast flow beads (GE) at 4 °C for 2 h. IgG beads were washed three times with lysis buffer, and proteins were eluted with 0.1 M glycine (pH 2.5). Proteins were then concentrated and separated by SurePAGE Gel (Genscript). Gels were stained with Coomassie Brilliant Blue, and in-gel digestion and liquid chromatography-tandem mass spectrometry analysis were performed according to a standard protocol as previously described (48). Data were analyzed with Turbo Sequest V2.7 software.

Coimmunoprecipitation. A total of 5×10^8 cells were harvested, washed with 1× phosphate buffer saline, and then lysed with glass beads in 0.4 mL lysis buffer (20 mM Hepes/KOH, pH 7.5, 150 mM NaCl, 0.5% Triton X-100, 10% glycerol, 1 mM $MgCl_2$, 1 mM PMSF, 1 μg/mL pepstatin, 1 μg/mL leupeptin; 1 μg/mL chymostatin; 125 U/mL benzonase nuclease; Sigma). The lysate was cleared by centrifugation at 13,000 × *g* for 5 min. A total of 30 μL of Protein A magnetic beads (MedChemExpress) and 4 μg Myc/FLAG antibody were added and incubated overnight at 4 °C. The magnetic beads were washed four times with lysis buffer and resuspended in 30 μL Laemmli buffer. The beads were heated at 95 °C for 3 min. Then samples were separated and detected by Western blot.

Western Blot. Yeast cells were lysed with glass beads in 20% trichloroacetic acid. The pellet was washed and proteins were extracted with Laemmli buffer. Protein samples were denatured in boiling water for 5 min and separated by sodium dodecyl sulfate polyacrylamide gel . The following antibodies were used for immunoblotting after membrane transfer: mouse monoclonal anti-HA (H3663, Sigma), mouse monoclonal anti-Myc (sc-40, Santa Cruz Biotechnology), mouse monoclonal anti-Flag (66008-3, Proteintech), mouse monoclonal anti-ubiquitin (P4G7, Santa Cruz Biotechnology), rabbit monoclonal anti-ubiquitin (linkage-specific K48) (ab140601, Abcam), rabbit monoclonal anti-Myc (2278, Cell Signaling Technology), rabbit polyclonal anti-Flag (PM020, MBL), rabbit polyclonal anti-SUMO (gift from Wei Li, Institute of Zoology, Chinese Academy of Sciences, Beijing 100101, China), and mouse monoclonal anti-PGK1 (ab113687, Abcam). Membranes were imaged with an Amersham Imager 680. Signal was quantified using Quantity One.

Yeast Two-Hybrid Assay. For Y2H assay, coding sequences of Pds5, Pre1, Rpn6, and Rpt2 were separately subcloned into the pGBKT7 plasmid. Coding sequences of Pds5, Cdc53, Skp1, and all 33 proteasome subunits were separately subcloned into the pGADT7 plasmid. The bait and prey plasmids were cotransformed into the Y2H gold strain and the interaction was tested on synthetic drop-out −Leu −Trp −His plates.

Chromosome Spread and Immunofluorescence. Samples collected from synchronized cultures at the appropriate time were used for cytological analysis. The synchronized yeast cells were processed with Zymolyase 100 T to get spheroplasts, which were spread on a clean microscopy slide with 1% Lipsol and fixed by 3% paraformaldehyde containing 3.4% sucrose (34). For immunostaining, slides were treated with 0.2% Photo-Flo for 30 s, transferred to Tris-buffered saline (TBS, pH 8.0) for 15 min. Then a drop of 1% bovine serum albumin was applied onto the slides and incubated at room temperature for 10 min. Slides were incubated with proper primary and secondary antibodies sequentially. Primary antibodies used in this study include mouse monoclonal anti-Myc (Santa Cruz Biotechnology), rabbit monoclonal anti-Myc (2278, Cell Signaling Technology), rabbit polyclonal anti-Flag (PM020, MBL), rat monoclonal anti-HA (11867423001, Roche), mouse monoclonal anti-ubiquitin (P4G7, Santa Cruz Biotechnology), goat polyclonal anti-Zip1 (sc-48716, Santa Cruz Biotechnology, anti-Zip1 N-terminal fragment), rabbit polyclonal anti-Zip1 C-terminal fragment (prepared by Dia-An Biotech, Inc., Wuhan, China), rat polyclonal anti-Pds5 (prepared by Dia-An Biotech, Inc.), mouse monoclonal anti-V5 (TransGen Biotech), rabbit polyclonal anti-GFP (a11122, Thermo Fisher Scientific), and rabbit polyclonal anti-SUMO (a gift from Wei Li). The following secondary antibodies were used in this study: Alexa 488–conjugated donkey anti-mouse/goat/rabbit (Thermo Fisher Scientific), DyLight 550–conjugated donkey anti-rat (Thermo Fisher Scientific), Alexa 555–conjugated donkey anti-rabbit (Thermo Fisher Scientific), Alexa 594–conjugated donkey anti-rat/goat (Thermo Fisher Scientific), and Alexa 647–conjugated donkey anti-goat or mouse (Thermo Fisher Scientific). Chromosomal DNA was stained by DAPI. Fluorescence images were visualized and acquired using a Zeiss fluorescence microscope AxioImager.Z2. Superresolution structured illumination microscopy analysis was performed using Acquire SR software on a DeltaVision OMX SR superresolution imaging system (GE Healthcare), and the images were further computationally reconstructed and processed with softWoRx software (GE Healthcare) to generate superresolution optical series sections.

Measurement of Chromosome Axis Length and Quantification of Immunofluorescence Intensity. Chromosome axis length can be accurately measured by immunostaining of axis component Rec8, Red1, or SC central element Zip1 (24). The fluorescence intensities were quantified as described previously (24). For quantification purposes, immunostaining and imaging were performed under the same condition including the same concentration for each antibody, the same incubation time and buffers, the same parameters in image acquisition, etc. The fluorescence intensity was quantified with ImageJ. To determine the background level, a chromosome fragment was randomly selected and a line perpendicular to it was drawn. The fluorescence intensity of each pixel of this line was shown as a normal distribution curve. The intensity of the pixel where the curve turns as a horizontal line was defined as background. Three chromosome fragments and thus three background values were determined per nucleus. The mean of the three background values was the background pixel intensity in that nucleus. To obtain the raw fluorescence intensity of a nucleus, a minimal circle was drawn to enclose the target nuclear area and the total intensity was measured by ImageJ as the raw intensity (signal at Zip1 polycomplex area was excluded). The total background for this nucleus was determined as the product of the background pixel intensity and area size (pixels). The fluorescence intensity was obtained by subtracting the background from the total fluorescence.

Chromosome Compaction Assay. Chromosome compaction was examined according to a previous description (33). Meiotic cells in SPM were collected at the indicated time. Cells were spread and stained with antibodies against Zip1 and GFP. The distances between the two GFP spots were measured by ImageJ software after imaging under a Zeiss fluorescence microscope AxioImager Z2. Cells were staged according to the morphologies of Zip1.

Quantification and Statistical Analysis. Data were analyzed with EXCEL or GraphPad Prism and presented as means ± SD, SEM, range, or 95% confidence interval as stated in the figure legends. Sample sizes, *n* values, are described in the figure legends. The Student's *t* test or two-proportion *z* test as indicated in the corresponding figure legends was performed to determine the levels of significance between two groups of samples. $P \geq 0.05$ (n.s., not significant), $^*P < 0.05$, $^{**}P < 0.01$, and $^{***}P < 0.001$.

Data Availability. All study data are included in the article and/or supporting information.

ACKNOWLEDGMENTS. We thank N. Kleckner for strains/plasmids and N. Kleckner and N. Hunter for discussion. This work was supported by the National Natural Science Foundation of China (31890782, 31900402, and 31771385), the National Key R&D Program of China (2018YFC1003700 and 2018YFC1003400), and the Taishan Scholars Youth Project of Shandong Province.

Author affiliations: [a]Center for Reproductive Medicine, School of Medicine, Cheeloo College of Medicine, Shandong University, Shandong 250012, China; [b]State Key Laboratory of Microbial Technology, Shandong University, Shandong 250012, China; [c]Development Center of Plant Germplasm Resources, College of Life and Environmental Sciences, Shanghai Normal University, Shanghai 200234, China; [d]National Research Center for Assisted Reproductive Technology and Reproductive Genetics, Shandong University, Shandong 250012, China; [e]Key Laboratory of Reproductive Endocrinology, Ministry of Education, Shandong University, Shandong 250001, China; [f]Shandong Provincial Clinical Research Center for Reproductive Health, Shandong University, Shandong 250012, China; [g]Advanced Medical Research Institute, Shandong University, Shandong 250012, China; and [h]Key Laboratory of Animal Resistance Biology of Shandong Province, Institute of Biomedical Sciences, College of Life Sciences, Shandong Normal University, Shandong 250014, China

1. N. Hunter, Meiotic recombination: The essence of heredity. *Cold Spring Harb. Perspect. Biol.* **7**, a016618 (2015).

2. D. Zickler, N. Kleckner, Recombination, pairing, and synapsis of homologs during meiosis. *Cold Spring Harb. Perspect. Biol.* **7**, a016626 (2015).

3. C. Veller, N. Kleckner, M. A. Nowak, A rigorous measure of genome-wide genetic shuffling that takes into account crossover positions and Mendel's second law. *Proc. Natl. Acad. Sci. U.S.A.* **116**, 1659–1668 (2019).
4. N. Kleckner, Chiasma formation: Chromatin/axis interplay and the role(s) of the synaptonemal complex. *Chromosoma* **115**, 175–194 (2006).
5. H. Murakami *et al.*, Multilayered mechanisms ensure that short chromosomes recombine in meiosis. *Nature* **582**, 124–128 (2020).
6. S. Gray, P. E. Cohen, Control of meiotic crossovers: From double-strand break formation to designation. *Annu. Rev. Genet.* **50**, 175–210 (2016).
7. M. E. Serrentino, E. Chaplais, V. Sommermeyer, V. Borde, Differential association of the conserved SUMO ligase Zip3 with meiotic double-strand break sites reveals regional variations in the outcome of meiotic recombination. *PLoS Genet.* **9**, e1003416 (2013).
8. S. Wang *et al.*, Inefficient crossover maturation underlies elevated aneuploidy in human female meiosis. *Cell* **168**, 977–989.e17 (2017).
9. S. Wang *et al.*, Per-nucleus crossover covariation and implications for evolution. *Cell* **177**, 326–338.e16 (2019).
10. S. Wang *et al.*, Crossover patterns under meiotic chromosome program. *Asian J. Androl.* **23**, 562–571 (2021).
11. S. Wang *et al.*, Crossover interference, crossover maturation, and human aneuploidy. *BioEssays* **41**, e1800221 (2019).
12. E. de Boer, A. J. Dietrich, C. Höög, P. Stam, C. Heyting, Meiotic interference among MLH1 foci requires neither an intact axial element structure nor full synapsis. *J. Cell Sci.* **120**, 731–736 (2007).
13. U. Biswas, M. Stevense, R. Jessberger, SMC1α substitutes for many meiotic functions of SMC1β but cannot protect telomeres from damage. *Curr. Biol.* **28**, 249–261.e4 (2018).
14. E. Revenkova *et al.*, Cohesin SMC1 beta is required for meiotic chromosome dynamics, sister chromatid cohesion and DNA recombination. *Nat. Cell Biol.* **6**, 555–562 (2004).
15. I. Novak *et al.*, Cohesin Smc1beta determines meiotic chromatin axis loop organization. *J. Cell Biol.* **180**, 83–90 (2008).
16. A. Ward, J. Hopkins, M. Mckay, S. Murray, P. W. Jordan, Genetic interactions between the meiosis-specific cohesin components, STAG3, REC8, and RAD21L. *G3 (Bethesda)* **6**, 1713–1724 (2016).
17. I. Sumara, E. Vorlaufer, C. Gieffers, B. H. Peters, J. M. Peters, Characterization of vertebrate cohesin complexes and their regulation in prophase. *J. Cell Biol.* **151**, 749–762 (2000).
18. Z. Zhang *et al.*, Budding yeast PDS5 plays an important role in meiosis and is required for sister chromatid cohesion. *Mol. Microbiol.* **56**, 670–680 (2005).
19. D. van Heemst, F. James, S. Pöggeler, V. Berteaux-Lecellier, D. Zickler, Spo76p is a conserved chromosome morphogenesis protein that links the mitotic and meiotic programs. *Cell* **98**, 261–271 (1999).
20. H. Jin, V. Guacci, H. G. Yu, Pds5 is required for homologue pairing and inhibits synapsis of sister chromatids during yeast meiosis. *J. Cell Biol.* **186**, 713–725 (2009).
21. D. Q. Ding *et al.*, Meiotic cohesins modulate chromosome compaction during meiotic prophase in fission yeast. *J. Cell Biol.* **174**, 499–508 (2006).
22. D. Q. Ding *et al.*, Meiotic cohesin-based chromosome structure is essential for homologous chromosome pairing in *Schizosaccharomyces pombe*. *Chromosoma* **125**, 205–214 (2016).
23. A. Viera *et al.*, PDS5 proteins regulate the length of axial elements and telomere integrity during male mouse meiosis. *EMBO Rep.* **21**, e49273 (2020).
24. M. Song *et al.*, Interplay between Pds5 and Rec8 in regulating chromosome axis length and crossover frequency. *Sci. Adv.* **7**, eabe7920 (2021).
25. C. H. Cheng *et al.*, SUMO modifications control assembly of synaptonemal complex and polycomplex in meiosis of *Saccharomyces cerevisiae*. *Genes Dev.* **20**, 2067–2081 (2006).
26. G. W. Hooker, G. S. Roeder, A role for SUMO in meiotic chromosome synapsis. *Curr. Biol.* **16**, 1238–1243 (2006).
27. J. S. Ahuja *et al.*, Control of meiotic pairing and recombination by chromosomally tethered 26S proteasome. *Science* **355**, 408–411 (2017).
28. H. B. Rao *et al.*, A SUMO-ubiquitin relay recruits proteasomes to chromosome axes to regulate meiotic recombination. *Science* **355**, 403–407 (2017).
29. N. R. Bhagwat *et al.*, SUMO is a pervasive regulator of meiosis. *eLife* **10**, e57720 (2021).
30. C. Liu *et al.*, Slx5p-Slx8p promotes accurate chromosome segregation by mediating the degradation of synaptonemal complex components during meiosis. *Adv. Sci. (Weinh.)* **7**, 1900739 (2020).
31. Z. Xu *et al.*, H2B ubiquitination regulates meiotic recombination by promoting chromatin relaxation. *Nucleic Acids Res.* **44**, 9681–9697 (2016).
32. L. Gómez-H *et al.*, The PSMA8 subunit of the spermatoproteasome is essential for proper meiotic exit and mouse fertility. *PLoS Genet.* **15**, e1008316 (2019).
33. Y. Wang *et al.*, ESA1 regulates meiotic chromosome axis and crossover frequency via acetylating histone H4. *Nucleic Acids Res.* **49**, 9353–9373 (2021).
34. L. Zhang *et al.*, Topoisomerase II mediates meiotic crossover interference. *Nature* **511**, 551–556 (2014).
35. I. Velichutina, P. L. Connerly, C. S. Arendt, X. Li, M. Hochstrasser, Plasticity in eucaryotic 20S proteasome ring assembly revealed by a subunit deletion in yeast. *EMBO J.* **23**, 500–510 (2004).
36. K. Voelkel-Meiman *et al.*, SUMO localizes to the central element of synaptonemal complex and is required for the full synapsis of meiotic chromosomes in budding yeast. *PLoS Genet.* **9**, e1003837 (2013).
37. Z. Zhu, M. Bani Ismail, M. Shinohara, A. Shinohara, SCF^{Cdc4} ubiquitin ligase regulates synaptonemal complex formation during meiosis. *Life Sci. Alliance* **4**, e202000933 (2020).
38. E. Alipour, J. F. Marko, Self-organization of domain structures by DNA-loop-extruding enzymes. *Nucleic Acids Res.* **40**, 11202–11212 (2012).
39. G. Fudenberg *et al.*, Formation of chromosomal domains by loop extrusion. *Cell Rep.* **15**, 2038–2049 (2016).
40. K. P. Kim *et al.*, Sister cohesion and structural axis components mediate homolog bias of meiotic recombination. *Cell* **143**, 924–937 (2010).
41. C. Grey, B. de Massy, Chromosome organization in early meiotic prophase. *Front. Cell Dev. Biol.* **9**, 688878 (2021).
42. P. Goetz, A. C. Chandley, R. M. Speed, Morphological and temporal sequence of meiotic prophase development at puberty in the male mouse. *J. Cell Sci.* **65**, 249–263 (1984).
43. W. M. Baarends *et al.*, Loss of HR6B ubiquitin-conjugating activity results in damaged synaptonemal complex structure and increased crossing-over frequency during the male meiotic prophase. *Mol. Cell. Biol.* **23**, 1151–1162 (2003).
44. H. Klug *et al.*, Ubc9 sumoylation controls SUMO chain formation and meiotic synapsis in *Saccharomyces cerevisiae*. *Mol. Cell* **50**, 625–636 (2013).
45. P. W. Brown, K. Hwang, P. N. Schlegel, P. L. Morris, Small ubiquitin-related modifier (SUMO)-1, SUMO-2/3 and SUMOylation are involved with centromeric heterochromatin of chromosomes 9 and 1 and proteins of the synaptonemal complex during meiosis in men. *Hum. Reprod.* **23**, 2850–2857 (2008).
46. A. De Muyt *et al.*, E3 ligase Hei10: A multifaceted structure-based signaling molecule with roles within and beyond meiosis. *Genes Dev.* **28**, 1111–1123 (2014).
47. P. Li, Y. Shao, H. Jin, H. G. Yu, Ndj1, a telomere-associated protein, regulates centrosome separation in budding yeast meiosis. *J. Cell Biol.* **209**, 247–259 (2015).
48. J. Wu *et al.*, Immune responsive release of tacrolimus to overcome organ transplant rejection. *Adv. Mater.* **30**, e1805018 (2018).